GROUP AND PHASE SPEED ANALYSIS FOR PREDICTING AND MITIGATING THE EFFECTS OF FLUCTUATIONS

W. A. KUPERMAN, S. KIM, G. F. EDELMANN, W. S. HODGKISS, AND H. C. SONG

Scripps Institution of Oceanography, University of California, San Diego, La Jolla, CA 92093-0701, USA, E-mail: [wak,seongil,geoff,wsh,hcsong]@mpl.ucsd.edu

T. AKAL *

SACLANT Undersea Research Centre,19138 La Spezia, Italy E-mail: tuakal@yahoo.com

The relationship between group and phase speed in an ocean waveguide is a robust descriptor of signal structure. Since different propagation paths or mode groups have characteristic group-phase speed relations (described by waveguide invariants), it turns out that this group-phase speed (g-p) structure is also useful for identifying the dominant fluctuating modal regions in, for example, shallow water internal wave fields. Since an acoustic time reversal mirror (TRM) works on a retransmission mechanism based on group speed structure (”last in, first out”), we will use TRM experimental results to illustrate the relation between acoustic fluctuations and g-p structure and to provide guidance for developing robust acoustic processing methods in fluctuating environments.

1 Introduction

It is well known that quantitative and qualitative information about sound propagation in a waveguide can be obtained by studying the modal (or ray) group speed (or cycle distance) and phase speed (or launch angle) relation which we term g-p structure. Much of this information is embedded in the waveguide invariant $[1,2,3,4]$. In this paper we relate the g-p structure to acoustic fluctuations, providing insight that can lead to signal processing methods that are robust in fluctuating environments. We will summarize the background theory and use results from recent time-reversal experiments (or phase conjugation in the frequency domain) $[5,6,7,8,9]$ to demonstrate the existence of simple robust diagnostics that ultimately guide us to stabilizing processing methods. The signal processing we suggest is then demonstrated by simulation.

2 Group and Phase Speed Structure in Shallow Water

For both reflection and refraction dominated propagation paths, phase speed increases with increasing launch angle. However, for reflection dominated paths, group speed decreases with increasing phase speeds whereas for refracting paths, group speed increases with increasing phase speed. These relations are summarized by the waveguide invariant for

*PRESENT ADDRESS: TUBITAK-MAN, MARMARA RESEARCH CENTER, EARTH AND MARINE SCIENCES RESEARCH INSTITUTE, P.K.21 GEBZE, KOCAELI 41470, TURKEY

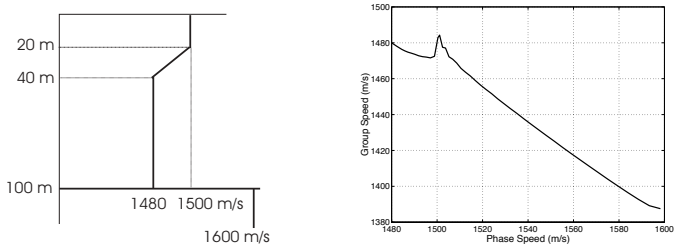

Figure 1. Group speed vs phase speed for an idealized summer profile (1000 Hz)

mode groups defined as $[1,2,3,4]$

$$\overline{\beta}_{nm} = -\frac{\Delta \overline{s}_{g,mn}}{\Delta s_{p,mn}}. \tag{1}$$

Here $\Delta \overline{s}_{g,mn} = \overline{s}_{g,m} - \overline{s}_{g,n}$ and $\Delta s_{p,mn} = s_{p,m} - s_{p,n}$. The $\overline{s}_{g,m}$ and $s_{p,m}$ are the m-th mode group and phase slowness, respectively. The upper bar means the range-averaged value in a range-dependent ocean environment. By mode groups we mean to include cases in a waveguide where both refracting and reflecting modes are present (e.g., summer profile where low modes are refracted below thermocline and higher modes are reflected at both boundaries); the demarcation between the mode groups varies with frequency.

We use a range-independent waveguide for our baseline environment. The invariant β describes the shift in the waveguide interference structure with respect to frequency through the relation (ignore the second term on the r.h.s of the equation for the time being)

$$\frac{\delta r}{r} = \frac{1}{\beta}\frac{\delta \omega}{\omega} - \frac{\gamma}{\beta}\frac{\delta h}{h}. \tag{2}$$

For example the peaks in the interference pattern at angular frequency ω as a function of range r are shifted by δr when the frequency under consideration is shifted by $\delta\omega$. Clearly the sign of β is important; β is typically positive for reflecting environments and negative for refracting environments $[1,2,4,10]$. One generalization to the waveguide invariant can be written down from Ref. $[3]$ which is given by all the terms in Eq. 2, where h is a duct thickness confining a particular mode group. For an ideal waveguide, $\beta = 1$ and $\gamma = -2$. Thus, increasing the channel depth shifts the interference pattern out to increasing range, a phenomenon measured during tidal variations and theoretically predicted from a simple perturbation analysis $[11]$. Though the result is simple, if one has a fixed receiver, this ebb and flow of the single frequency interference pattern appears as an almost random fluctuation though a spectrogram (intensity vs ω and time) would show a distinct pattern. These type of fluctuations have also been addressed in terms of waveguide invariants both theoretically and experimentally, the latter using the frequency-time diversity of FM sweeps $[12,13,14,15]$.

With simple group and phase speed arguments, we can identify two types of fluctuations:

1. The first can be thought of as the result of an ebb and flow of modes. If the modes stay within groups with the same invariant quantity, the flow is similar to the tidal variation example discussed above.

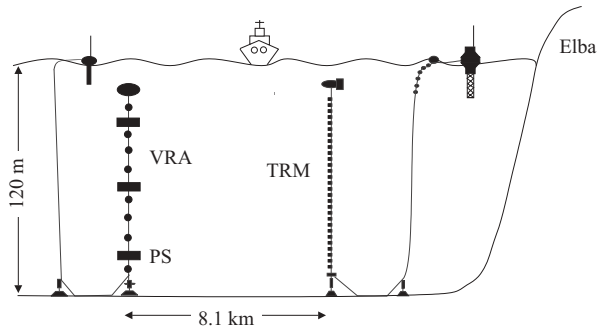

Figure 2. Schematic of TRM experiment. The prope source (PS) is attached to a vertical receive array (VRA) which sample the backpropagated pulse at the focal distance.

2. The other type is from a modal transition region [16] where the nature of a mode changes, for example, a case when a refracted mode changes to a reflected mode. This can happen for a summer profile where the next mode after the highest mode refracted below the thermocline is now surface reflected. Such a transition, would also occur for a given mode in the transition region by going from a higher to lower frequency (cutoff from refracting to reflecting ducts). By virtue of the generalized waveguide invariant above, this process would occur at a given frequency by a change in the refracting duct size as could be caused by internal waves.

Examine Fig. 1 which is a g-p phase speed plot of an idealized summer profile environment. It is where there is an abrupt change in the sound speed profile where internal waves have the maximum amplitude. For a ray turning around (mode is evanescent) in the phase speed region around 1500 m/s, we see a maximum variation in group speed; in this region there will be fluctuations between different modes (phase speeds) with the same group velocity. The fluctuation is between refracting and reflecting paths and therefore is in the region where β is changing sign (slope reversals in g-p curves). A time reversal experiment would emphasize these two phenomena since the first-in last-out processing would fluctuate between the spatial structure of the incoming field and one in which the modes are scrambed in the transition region (i.e., same modes transitioning to other group speeds and modes at the same group speed being redistributed about the local maximum).

3 Performance of a Time Reversal Mirror in Fluctuating Environments

We have already reported on a series of Time Reversal Mirror (TRM) experiments [5, 6, 7, 8, 9]. Figure 2 shows the basic geometry of these experiments. The probe source (PS) transmits a signal to the TRM where it is time reversed and retransmitted; a focus is produced at the PS if the forward and backpropagating environments are the same. Figure 3 shows the environments of the last experiment and the computed g-p curves. By the arguments above, one should be able to determine which environments would support time reversal (minimal fluctuation between forward and backpropagating time intervals). For example, station 1 shows a very unstable profile with many slope reversals whereas the station 9 is stable up to the phase speed of 1520 m/s corresponding to the maximum propagating mode. Indeed, the acoustic data verified this relation between stability and

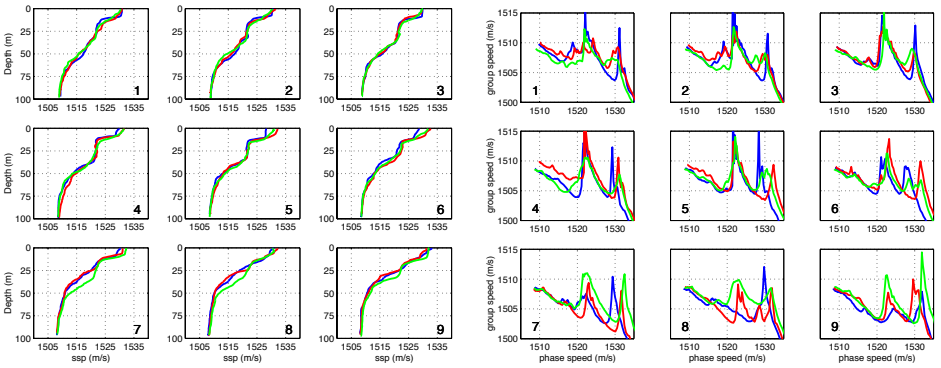

Figure 3. Sound speed profiles on three consecutive days at nine different positions north of Elba and corresponding gp curves

g-p curves to the point that by just measuring the sound speed profile and making the g-p computation, we could predict when time reversal would be robust or problematic.

Now we go to a case where we examine the fluctuating focus as a function of time. Figure 4 is an example of a single TRM result and Fig. 5 shows a sequence of TRM foci for which the same probe source signal at the TRM was retransmitted every minute for 50 minutes. In this particular one of many examples, the focus degrades considerably after 10 minutes but reappears after 40 minutes. What we would like is a signal processing method which stabilizes the focus.

4 Mitigating Fluctuation Effects by Adaptive Processing

Phase conjugation and matched field processing (MFP) are closely related [17], the latter using a computer simulation (replicas) for backpropagation. For MFP, an assortmnt of robust algorithms have been proposed [18]. The sound speed perturbation method (MSC) [19] based on multi-constraint array processing methods (MLC) [20] appears promising and more or less uses replica vectors obtained from a singular value decomposition (SVD)

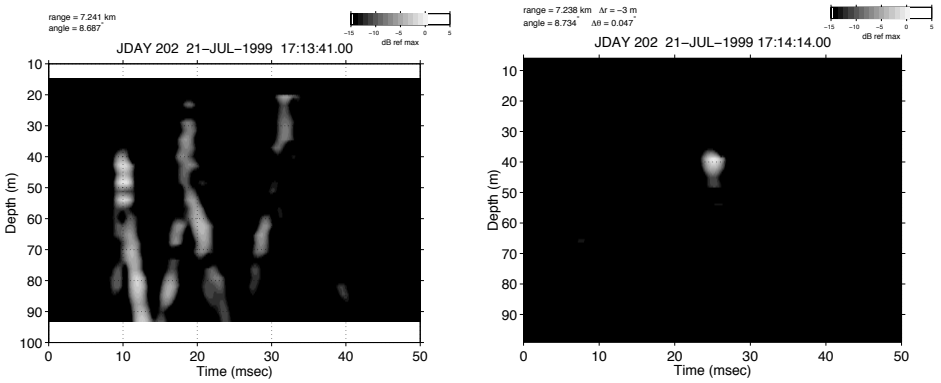

Figure 4. Multipath signal received by the TRM (left) and refocused signal at the original PS location (right)

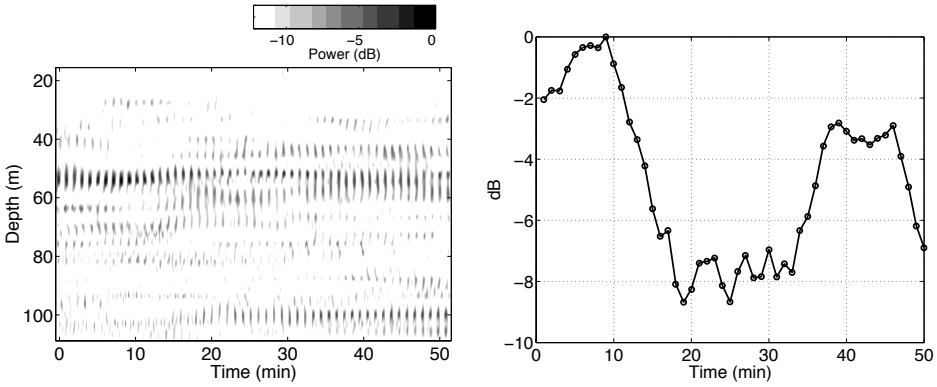

Figure 5. Measured time reversal stability with 3.5 kHz transmissions: sequence of TRM foci due to the same probe signal transmitted every minute for 50 minutes (left) and variation of the intensity level at the PS positions (right)

of a large matrix representing an ensemble of environments. From Eq. 2, we can think of the frequency bins of a pulse as containing acoustic information representing different ranges and/or environmental realizations. The frequency-range shift has alread been verified by TRM experiments [7]. Hence, based on Ref. [19], we propose the following multi-frequency constraint (MFC) procedure [9]:

The first step is constructing a probe signal matrix by from probe signal vectors as

$$\mathbf{P} = [\mathbf{p}_1, \mathbf{p}_2, \cdots, \mathbf{p}_N], \tag{3}$$

where $\mathbf{P}$ is a $J \times N$ probe signal matrix at frequency ω and each element $\mathbf{p}_n$ is a $J \times 1$ signal vector. J is the number of transducers in the TRM and N is the number of probe signal vectors received by the TRM, each corresponding to a frequency component extracted from a broadband pulse

$$\mathbf{p}_n = G(\mathbf{r}_j; \mathbf{r}_s, t_1, \omega_n), \tag{4}$$

where ω_n is a frequency bin around ω. The performance of the adaptive method depends on how well signal matrix constructed by the multiple frequency bin vectors spans the ensemble of backpropagating environments as per the physics of Eq. 2.

Next, we adopt the arguments and procedure described in Ref. [19] to the frequency vectors hypothesized to span the environmental ensemble as estimated from the generalized waveguide invariant: If we take many frequency bins, the number of vectors spanning all possible wave-front perturbations can be large but the modal phase perturbations can be highly correlated among the modes as well as signal pings. The dimension actually is determined by the number of effective internal wave modes interacting with acoustic modes. Normally, internal waves can be represented by a few modes in shallow water [21]. The design of an efficient constraint space for the signal vector consists of selecting the minimum number of vectors that can best approximate the phase perturbation space. This order reduction can be achieved using the singular value decomposition of the signal matrix $\mathbf{P}$ with a rank K approximation,

$$\mathbf{P}(\omega) \simeq \mathbf{U}\Sigma\mathbf{V}^{\dagger}, \tag{5}$$

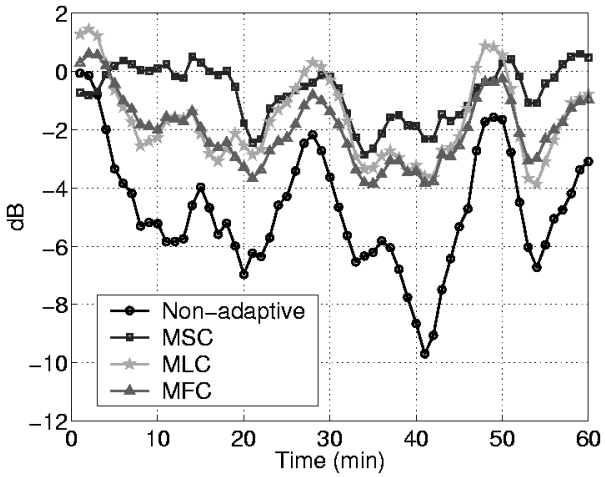

Figure 6. Simulated time-reversal focal strength using various adaptive methods: multiple sound speed constraints (MSC), multiple location constraints (MLC), and multiple frequency constraints (MFC).

where †is the Hermition transpose, $\mathbf{U}$ is a $J \times K$ matrix whose columns are the left singular vectors, Σ is a $K \times K$ matrix whose diagonal elements are the singular values of $\mathbf{P}$, and $\mathbf{V}$ is a $N \times K$ matrix whose columns are the right singular vectors. Now the field vector $\mathbf{H}$ for backpropagation is obtained by the linear combination of left singular vectors,

$$\mathbf{H}(\omega) = \mathbf{U}(\omega)\mathbf{q}, \tag{6}$$

where $\mathbf{q}$ is a $K \times 1$ vector representing the coefficient used for the linear combination of the singular vectors. We expect the singular values to decrease rapidly with increasing number so that in many cases the first singular vector corresponding to the largest singular value is sufficient as a field vector for stable focusing. In this case $\mathbf{q} = [1, 0, \ldots, 0]^T$.

The final step is replacing $G(\mathbf{r}_j; \mathbf{r}_s, t_1, \omega)$ for the data on the TRM so that the adaptive time-reversed pressure field becomes

$$p_{tr}(\mathbf{r}, t_2, \omega) = \sum_j S^*(\omega) H^*(\mathbf{r}_j, \omega) G(\mathbf{r}; \mathbf{r}_j, t_2, \omega). \tag{7}$$

Here a new source spectrum $S(\omega)$ is inserted in the backpropagation which can have a different shape from the original source spectrum used for the probe source signal. This process should exhibit a stable focal structure since the field vector $H(\mathbf{r}_j, \omega)$ was designed to maintain high correlation with $G(\mathbf{r}; \mathbf{r}_j, t_2, \omega)$ for all possible wave-front perturbations. This leads to increased focal sizes and a stable focus since in most cases, higher order modes, and in particular, those representing rays that turn in the internal wave regions are de-emphasized.

This algorithm was motivated by the data in our TRM experiments but developed after the last experiment. Therefore we must use simulation to demonstrate its effectiveness. Figure 6 shows a simulation of the data from a TRM experiment exhibiting much

of the same behavior of the data shown in Fig. 5. Internal wave simulations were based on Ref [21, 22] and the broadband normal propagation utilized Ref. [23]. Figure 6 also shows an application of the MFC algorithm together with the two other algorithms, MSC and MLC of Refs. [19, 20] where the latter two methods require an additional (and impractical) large amount of data – multiple pings or multiple probe source locations [9]. The stabilization of the TRM focus is quite evident.

5 Conclusion

In this paper we reviewed how group and phase speed (g-p) structure as summarized by the generalized waveguide invariant relates environment to the space-time-frequency structure of a propagating signal. We then showed that our stability results from TRM experiments were consistent with our interpretation of the g-p structure. Basically, in this picture, environmental fluctuations have acoustic trajectories in the multidimensional space-time-frequency space and we normally sense these fluctuations in one of the basis planes (e.g., space-time) – possibly and unintentionally maximizing the appearance and effect of fluctuations. Our understanding of frequency-range shift caused by the environment through the generalized waveguide invariant concept then provides guidance to construct an adaptive procedure to stabilize the focal structure of a TRM in a flucutating environment. The proposed processing was successfully demonstrated with simulation and the method, by virtue of its derivation, should also be applicaple to MFP.

Acknowledgements

This research was supported by the U. S. Office of Naval Research.

References

1. S. D. Chuprov, "Interference structure of a sound field in a layered ocean," in *Acoustics of the Ocean*, edited by L. M. Breakhovskikh and I. B. Andreevoi, Nauka, Moscow, 71–91, 1982.
2. L. M. Brekhovskikh and Y. P. Lysanov, *Fundamentals of ocean acoustics*, Springer, 1991.
3. G. A. Grachev, "Theory of acoustic field invariants in layered waveguide," *Acoust. Phys.*, 39(1), 33–35, 1993.
4. G. L. D'Spain and W. A. Kuperman, "Application of waveguide invariants to analysis of spectrograms from shallow water environments that vary in range and azimuth," *J. Acoust.Soc. Am.*, 106, 2454–2468, 1999.
5. W. A. Kuperman, W. S. Hodgkiss, H. C. Song, T. Akal, C. Ferla, and D. Jackson, "Phase conjugation in the ocean: Experimental demonstration of an acoustic time-reversal mirror," *J. Acoust. Soc. Am.*, 102, 25–40,1998.
6. W. S. Hodgkiss and H. C. Song, W. A. Kuperman, T. Akal, C. Ferla, and D. R. Jackson, "A long range and variable focus phase conjugation experiment in shallow water," *J. Acoust. Soc. Am.*,105,1597–1604, 1999.
7. H. C. Song, W. A. Kuperman, and W. S. Hodgkiss, "A time-reversal mirror with variable range focusing," *J. Acoust. Soc. Am.*, 103, 3234–3240,1998.
8. S. Kim, G. F. Edelmann, W. A. Kuperman, W. S. Hodgkiss, H. C. Song, and T. Akal, "Spatial resolution of time-reversal arrays in shallow water," *J. Acoust. Soc. Am.*, 110, 820–829,2001.
9. S. Kim, W. A. Kuperman, W. S. Hodgkiss, H. C. Song, G. F. Edelmann, and T. Akal, "Adaptive time reversal for robust focusing in the ocean," submitted to *J. Acoust. Soc. Am.* 2002.

10. G. L. D'Spain, J. J. Murray, W. S. Hodgkiss, N. O. Booth, and P. W. Schey, "Mirages in shallow water matched filed processing," *J. Acoust.Soc. Am.*, 105, 3245–3265, 1999.
11. D. E. Weston and K. J. Stevens, "Interference of wide-band sound in shallow water," *J. Sound and Vibration*, 21, 57–64, 1972.
12. V. M. Kuz'kin, "The effect of variability of ocean stratification on a sound field interference structure," *Acoust. Phys.*, 41, 300–301, 1995.
13. V. M. Kuz'kin, A. V. Ogurtsov, and V. G. Petnikov, "The effect of hydrodynamic variability on frequency shifts of the interference pattern of a sound field in a shallow water sea," *Acoust. Phys.*, 44, 77–82, 1998.
14. V. M. Kuz'kin, "Frequency shifts on the sound field interference pattern in a shallow water," *Acoust. Phys.*, 45, 224–229, 1998.
15. , V. G. Petnikov and V. M. Kuz'kin, "Shallow water variability and its manifestation in interference pattern of sound field," in *Ocean acoustic interference phenomena and signal processing*, edited by W. A. Kuperman and G. L. D'Spain, AIP Press, New York, 2002.
16. W. A. Kuperman, G. L. D'Spain and K. D. Heaney,"Long range source localization from single hydrophone spectrograms" *J. Acoust. Soc. Am.*, 109, 1934–1943, 2001.
17. W. A. Kuperman and D. R. Jackson, "Ocean acoustics, matched-field processing and phase conjugation" in *Imaging of complex media with acoustic and seismic waves in Topics Appl. Phys.*, edited by Fink *et al*, Springer-Verlag, Berlin Heidelberg, 84, 43–97, 2002.
18. A. B. Baggeroer, W. A. Kuperman and P. N. Mikhalevsky, "An overview of matched field methods in ocean acoustics," *IEEE J. Oceanic Eng.*, 18, 401–424, 1993.
19. J. L. Krolik, "Matched-field minimum variance beamforming in a random ocean channel," *J. Acoust. Soc. Am.*, 92, 1408–1419, 1992.
20. H. Schmidt, A. B. Baggeroer, W. A. Kuperman, and E. K. Scheer, "Environmentally tolerant beamforming for high-resolution matched field processing: Deterministic mismatch," *J. Acoust. Soc. Am.*, 88, 1851–1862, 1990.
21. T. C. Yang and K. Yoo, "Internal wave spectrum in shallow water: Measurement and comparison with the Garrett-Munk model," *IEEE J. Ocean. Eng.*, 24, 333–345, 1999.
22. F. S. Henyey, D. Rouseff, J. M. Grochocinski, S. A. Reynolds, K. L. Williams, and T. E. Ewart, "Effects of internal waves and turbulence on a horizontal aperture sonar," *IEEE J. Oceanic Eng.*, 22, 270–280, 1997.
23. E. K. Westwood, C. T. Tindle and N. R. Chapman, "A normal mode model for acousto-elastic environments," *J. Acoust. Soc. Am.*, 100, 3631-3645,1996.